



REVIEW ARTICLE

Open Access



Structural diversity of natural cellulose and related applications using delignified wood

Yoshiki Horikawa*

Abstract

Cellulose is synthesized by organisms belonging to each biological kingdom, from bacteria to terrestrial plants, leading to its global-scale distribution. However, the structural properties of cellulose, such as its microfibril size, crystal form, cross-sectional shape, and uniplanar orientation, vary among species. This mini-review discusses the structural properties and diversity of cellulose. After describing historical developments in the structural analysis of cellulose, the technique of intracrystalline deuteration and rehydrogenation to understand structural diversity—particularly the localization of crystalline allomorphs in single microfibril—is discussed. Furthermore, the development of cellulose materials that maintain hierarchical structures of wood is introduced, and methods for producing functional materials are presented.

Keywords: Cellulose microfibril, Crystalline allomorphs, Uniplanar orientation, Intracrystalline deuteration, Infrared spectroscopy, Hierarchical structure

Introduction

Cellulose is the most abundant organic material on Earth, with 10^{11} – 10^{12} tons produced each year, primarily from water and carbon dioxide by plant photosynthesis [1]; it has recently attracted considerable attention as a renewable material to replace fossil-based resources. Cellulose is a major component of wood, which is packed into crystalline fibers referred to as “microfibrils” that align to form oriented sheets. A lamellar structure, which is based on piled sheets, forms the cell wall, and cells arrange to form the anatomical structure of wood. The combination of this sophisticated hierarchical structure with matrix components such as hemicellulose and lignin provides trees with the mechanical properties that enable them to grow large in size and live for long periods of time.

Many organisms other than trees, including sea algae, ascidians, and bacteria such as *Acetobacter*, also synthesize cellulose; however, cellulose suprastructures (e.g., crystalline form, cross-sectional shape, and in-plane

orientation) are highly diverse. This mini-review focuses on the structural diversity of natural cellulose and how historical developments have shaped our understanding of the cellulose structure. The intracrystalline deuteration technique that is used to evaluate structural diversity and methods for removing matrix components while maintaining the hierarchical structure of wood are also discussed in relation to their associated physical properties.

Crystalline allomorphs and their diversity

The Japanese researchers Nishikawa and Ono first identified the crystal formation of cellulose by irradiating wood, hemp, and bamboo with X-rays in 1913 to produce diffraction images [2]. Given that Laue had only recently discovered that X-rays produce diffraction patterns in 1912—by demonstrating that crystals are made up of periodic structures with intervals comparable to the wavelength of an X-ray—one can appreciate how both of these Japanese researchers made significant pioneering contributions to cellulose research. Subsequently, the active employment of X-ray diffractometry to obtain the first crystal model of cellulose was not reported until 1928 by Meyer and Mark [3], in which they proposed a

*Correspondence: horikawa@cc.tuat.ac.jp

Institute of Agriculture, Tokyo University of Agriculture and Technology, Fuchu, Tokyo 183-8509, Japan

parallel-chain structure with two molecular chains of the same orientation packed in a unit lattice. Since then, various unit lattices have been proposed, including the antiparallel chain model of Meyer and Misch in 1937 that involved two molecular chains face away from each other [4], and the eight-chain unit cell reported by Honjo and Watanabe two decades later [5]. Unfortunately, these models did not lead to the establishment of a widely accepted unified model.

The use of infrared (IR) spectroscopy, however, revealed that cellulose from sea algae and bacteria contain groups that differ from those of cotton and ramie, leading to the further classification of cellulose I as cellulose IA and IB [6, 7]. Fisher and Mann [8] examined the packing of molecular chains and found that the crystal lattices of cellulose IA and IB were different. Consequently, it remained a point of contention whether a unified model with the same structure for all natural celluloses or one with variations among species should be accepted. In 1974, a parallel-chain model was proposed using a combination of computerized refinement and energy calculations based on diffraction intensities, which was widely accepted as the crystal model for cellulose [9, 10]. However, it was not until the 1980s when solid-state nuclear magnetic resonance (NMR) spectroscopy became available that a model corresponding to cellulose IA and IB was proposed, leading to a new phase of cellulose structural studies. In other words, the IA and IB natural classifications of cellulose I were abandoned in favor of a mixture of I_α and I_β , the ratio of which varies among species [11, 12]. These two types of cellulose were broadly classified into the sea algae/bacteria type, in which I_α constitutes the majority, and the cotton/ramie type, which contains a large amount of I_β . Moreover, I_α cellulose can be converted into I_β by hydrothermal treatment [13] or high-temperature treatment in organic solvents and helium gas [14], which revealed that the I_β phase is more physically stable.

In 1991, the electron diffraction patterns obtained from a single microfibril before (I_α -rich) and after (I_β -dominant) hydrothermal treatment were analyzed, resulting in the proposed crystal models of single-chain triclinic and double-chain monoclinic unit cells corresponding to the I_α and I_β forms [15]. The precise structures of native celluloses have since been determined by synchrotron X-ray and neutron diffractometry [16, 17]. The presence of I_α and I_β can also be determined using IR spectroscopy [18], whereby cellulose I_α exhibits characteristic IR absorptions at 3240 and 750 cm^{-1} , while I_β exhibits bands at 3270 and 710 cm^{-1} . Although it is not clear which cellulose crystal lattice is the dominant form in wood due to its low crystallinity, a multifaceted analysis relying on a combination of IR, NMR,

X-ray, and electron diffraction techniques revealed that I_β dominates both the poplar xylem wall and gelatin layer [19]. Ascidiaceans are the only animal species that synthesize cellulose, predominantly as cellulose I_β . Interestingly, it was discovered that the type of cellulose differed between ascidian larvae and adults, which synthesize I_α and I_β , respectively [20]. Furthermore, separate synthetic genes were found to be involved, thus indicating that crystal structure formation is molecularly regulated in this animal. More recently, near-infrared spectroscopy [21] and terahertz time-domain spectroscopy [22] have been employed to evaluate cellulose structure in terms of its allomorphs.


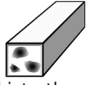
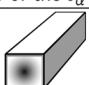
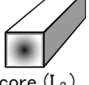
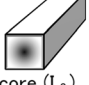

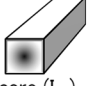
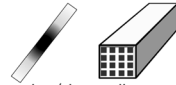
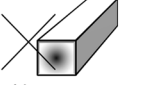
Localization of cellulose allomorphs within a single microfibril

Table 1 summarizes the proposed microfibril domain distribution models. The micro-electron diffraction method was first suggested to model the localization of each allomorph along the fiber axis based on the diffraction pattern of a single cellulose microfibril that was continuously followed [15]. In addition, detailed analyses of electron diffraction data obtained from several species of green algae led to the conclusion that the I_α and I_β domains are alternately/laterally localized in the microfibril direction [23].

An alternative model in which I_β is distributed in the center of the microfibril crystal and I_α on the crystal surface (the “skin (I_α)-core (I_β) structure”) was also proposed based on the concept that I_α , a metastable structure, is formed on the crystal surface under shear stress resulting from torsion associated with the bacterial cellulose ribbon [24]. Acid hydrolysis revealed microfibrils with sharp tips rich in I_β [25], suggesting that the I_α domains on the crystal surface are preferentially acid-hydrolyzed, leading to the skin (I_α)-core (I_β) structure for green alga cellulose.

As was observed during acid hydrolysis, I_α is more susceptible to degradation than I_β during enzymatic treatment [26, 27]. The same research group also observed microblock exfoliation from microfibrils in enzyme-treated *Cladophora* cellulose by atomic force microscopy [28], which led to the conclusion that the crystalline allomorphs are longitudinally localized rather than horizontally distributed. The formation of I_β -rich products with smaller microfibrils during treatment also supports a model in which I_β domains are surrounded by I_α in the microblocks that form the microfibrils. Interestingly, this model is similar to that in which I_β domains are packed inside I_α superlattices. In addition, I_β -rich cellulose is synthesized when acetic acid bacteria are grown in the presence of hemicellulose [29].

Table 1. Proposed models for localization of cellulose allomorphs within a single microfibril

Proposed model	Treatment	Method	Origin	Year	Reference
 Alternately		Electron microdiffraction	<i>Microdictyon</i>	1991	15
 I_β packed into the superlattice of the I_α	Culture with hemicellulose	NMR	Bacterial cellulose	1994	29
 Skin (I_α)-core (I_β)		IR, NMR	Bacterial cellulose	1996	24
 Skin (I_α)-core (I_β)	Enzymatic hydrolysis	Electron diffraction, IR, X-ray	<i>Cladophora</i>	1997	26
 Skin (I_α)-core (I_β)	Enzymatic hydrolysis	IR, X-ray	Bacterial cellulose <i>Valonia</i> <i>Cladophora</i>	1997	27
 Alternately / laterally		Electron microdiffraction, IR	<i>Boergesenia</i> <i>Cladophora</i> <i>Valonia</i>	1998	23
 Skin (I_α)-core (I_β)	Acid hydrolysis	IR, TEM imaging, X-ray	<i>Cladophora</i>	2001	25
 Alternately / laterally	Enzymatic hydrolysis	AFM imaging, IR	<i>Cladophora</i>	2005	28
 Not skin-core	Intracrystalline deuteration/rehydrogenation	IR	<i>Boergesenia</i> <i>Cladophora</i> <i>Valonia</i>	2008	49

Cross-sectional shape of microfibrils

In order to discuss the natural cross-sectional shape diversity of microfibrils, an understanding of the method used for observing microfibril cross-sections must be mentioned first. Negatively stained transverse ultrathin sections can be imaged using electron microscopy by tilting them in various directions and at various angles [30]. The diffraction contrast method employed by Revol et al. [31] can be used for both bright-field imaging (in which all diffracted waves from the crystal are cut off by an objective aperture) and dark-field imaging (in which only diffracted waves are observed), allowing the cross-sectional shape to be determined without any need for staining.

The actual cross-sectional shape of *Valonia* cellulose microfibrils is square (approximately 20×20 nm) or rectangle [32]—similar cross-sectional shapes are observed for *Oocystis* and *Glaucocystis* [33]. However,

natural celluloses with cross-sections that are neither square nor rectangular have also been observed. For example, *Micrasterias*, a type of aquatic algae belonging to the Zygnematales order, has a very flat microfibril cross-section [34], while ascidians have unique parallelogram- or rhomboid-shaped microfibril cross-sections [35]. The actual cross-sectional shape of wood cellulose in the gelatin layer of poplar tension wood was reported to be square (approximately 3×3 nm) [36]. Recent advances in scattering and imaging techniques have led to an active debate on the cross-sectional shape of microfibrils in terrestrial plants. Spectroscopic methods coupled with small-angle neutron and wide-angle X-ray scattering have suggested a “rectangular” model for microfibrils [37], while computer-simulated analyses of wide-angle X-ray scattering data resulted in a variety of microfibril models [38]. Furthermore, Daicho et al. [39] proposed a hexagonal model with

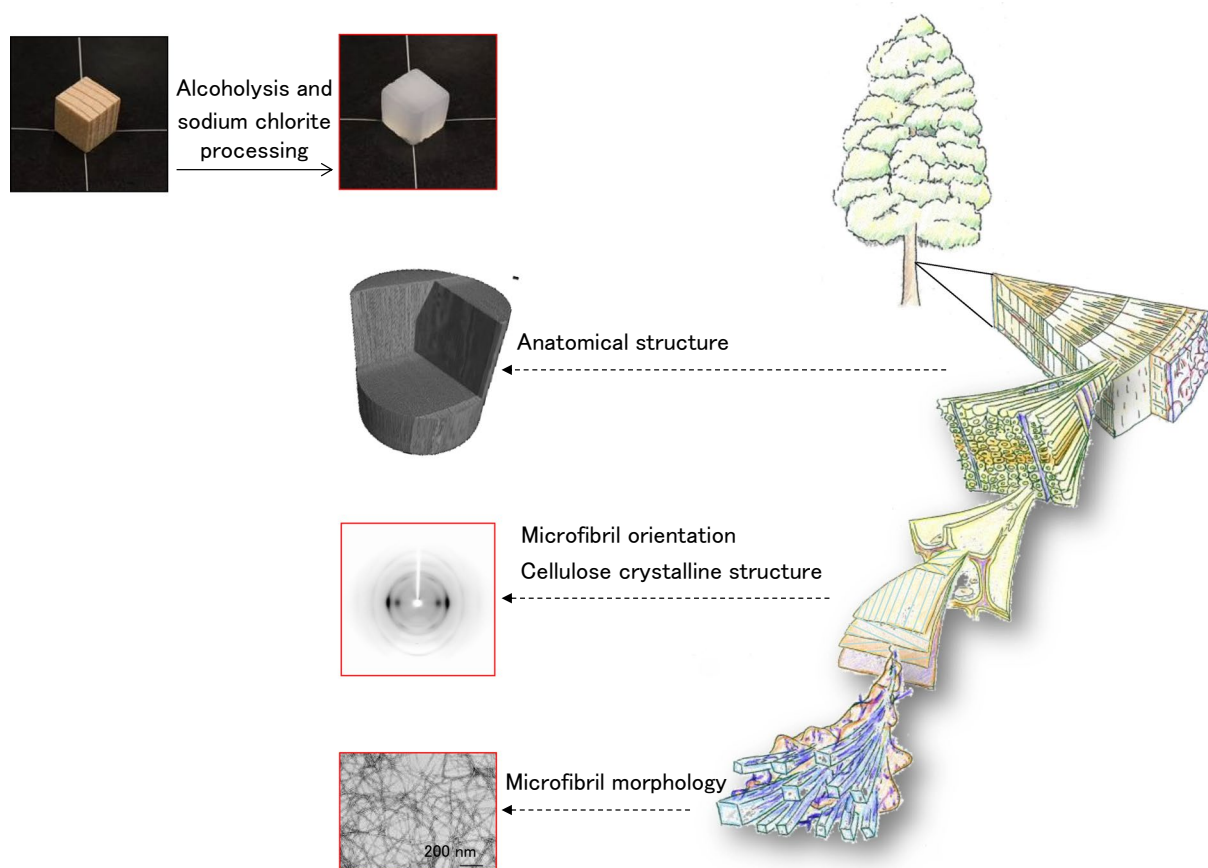


Fig. 1 Development of colorless wood by two-step delignification and structural analysis of the hierarchical architecture (reproduced from [70])

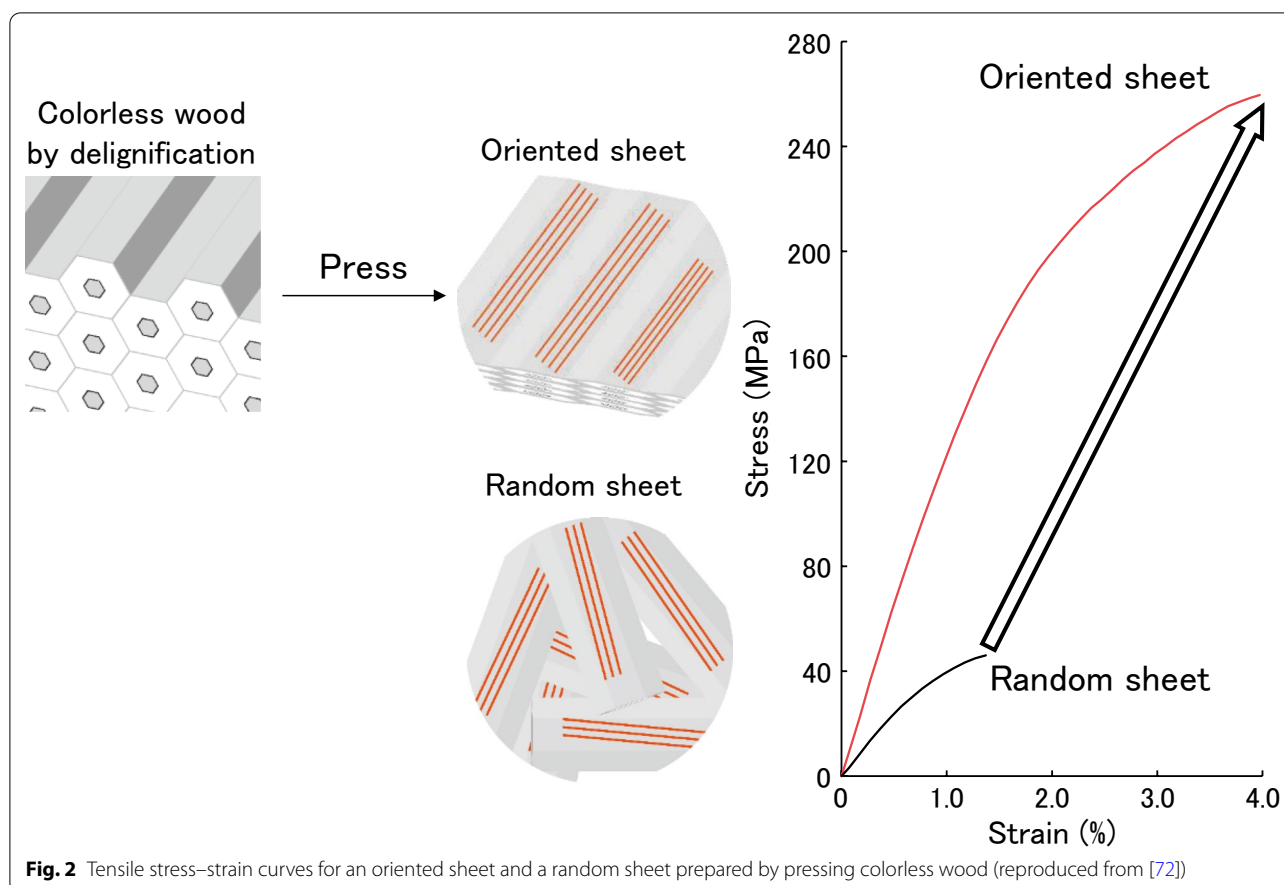
boundary faces parallel to all three reflection planes of $(1\bar{1}0)$, (110) , and (200) .

Preferential uniplanar orientation

The cell wall of *Valonia*, a green alga, has a crossed-lamellar structure. In other words, microfibrils within one lamella are deposited in a parallel arrangement, whereas those in adjacent lamellae are orthogonal. The microfibrils in both lamellae are oriented on a $0.60\text{--}0.61\text{ nm}$ plane [the (100) plane in I_α and the $(1\bar{1}0)$ plane in I_β] parallel to the cell membrane surface. In fact, the $0.53\text{--}0.54\text{ nm}$ plane [the (010) plane in I_α and the (110) plane in I_β] in the *Valonia* cell wall exhibits a more intense peak than the 0.61 nm plane by transmission X-ray diffractometry, which indicates that the 0.61 nm plane is deposited parallel to the cell wall. In addition to the *Valonia* cell structure, there is a type of structure in which microfibrils are deposited with a 90° rotation;

i.e., the $0.53\text{--}0.54\text{ nm}$ plane is oriented with the plasma membrane. The majority of microfibrils must be similarly oriented and individual microfibrils must also remain untwisted to observe a planar orientation. Consequently, rigid microfibrils with large fiber diameters and rectangular cross-sections adopt such orientations, which are common except among terrestrial plants. Ascidian [16] and bacterial [40] celluloses have been identified as types in which microfibrils are synthesized with a 0.61 nm planar orientation, as observed for *Valonia*. In contrast, the cellulose of *Glaucozystis* [33] is characterized by a plane-oriented 0.53 nm plane, as are celluloses from aquatic algae belonging to the Zygnematales order, such as *Spirogyra* [41], *Closterium* [42], and *Micrasterias* [34].

There are also types of cellulose that do not exhibit preferential uniplanar orientation, characterized by smaller microfibrils with individual microfibril torsion responsible for the lack of facial orientation; those of higher plants are included in this group. Packing energy



calculations [9] have revealed that cellulose molecules are stable in a state slightly divergent from the twofold helix; i.e., in a twisted state. In other words, hydrophobic and hydrogen bonding interactions within a crystal are less constrained for small microfibrils, leading to a loosely twisted fibril overall.

Intracrystalline deuteration and rehydrogenation for evaluating cellulose structural diversity

Deuteration can be employed to determine the accessibilities of cellulose microfibrils and other organic macromolecules because the hydrogen involved in hydrogen bonding can be replaced by deuterium. The early literature reports the immersion of cellulose specimens in D_2O , using weight differences to calculate the crystallinity, and in turn determine the structural accessibility [43]. Moreover, deuterium is useful in IR spectroscopy because the hydrogen/deuterium mass difference dramatically affects molecular vibrational frequencies, which for cellulose results in O–D bond vibrations that are located in spectral regions free from other absorbances. An IR spectrum acquired

immediately after exposure of a deuterated specimen to air exhibits strong O–D bands that weaken over time owing to D/H exchange with moisture in the air.

A significant achievement was reported in 1997 in which high-temperature annealing at 260 °C in 0.1 N NaOD resulted in deuterium exchange on the microfibril surface as well as in the crystalline core without damaging the crystalline structure [44]. Despite prolonged exposure to air, rehydrogenation occurred only on the surface of the specimen, with the core remaining deuterated. By lowering the annealing temperature of the intracrystalline deuteration technique to 210 °C [45], the initial crystalline allomorph persisted, thus facilitating investigations of completely deuterated I_α and I_β crystals separately and allowing for the precise refinement of hydrogen bonding networks of cellulose I allomorphs [16, 17].

Author and co-workers modified this intracrystalline deuteration technique to establish a stable and reproducible method to initially deuterate all of the primary hydrogen groups completely. The deuterated samples are then rehydrogenated by immersion in water at room temperature, whereby the deuterium atoms of all

surface OD groups are exchanged for protons to form OH groups [46]. This behavior during rehydrogenation at elevated temperatures confers accessibility to the crystal core, thereby providing important information on microfibril dimensions [47] and uniplanar orientation [48]. In addition, monitoring exchange behavior by observing characteristic IR absorbances on I_α and I_β during intracrystalline deuteration/rehydrogenation revealed that the I_α domain is localized on the surface as well as in the central core of the cellulose microfibril; therefore, the triclinic and monoclinic domains cannot be explained only in terms of a simple “skin–core” structure (Table 1) [49]. Recently, Funahashi et al. [50] developed a technique for peeling molecular chains from the surface of cellulose microfibrils in a layer-by-layer manner; this technique may provide new insights into the localization of cellulose allomorphs within a single microfibril.

Delignification with maintained hierarchical structures

Cellulose nanofibers are expected to be next-generation building blocks for the development of new materials because they are light and strong, with high elastic moduli and low linear expansion coefficients [51]. Various approaches have been developed to fabricate nanofibers, such as mechanical processing by grinding [52], aqueous counter collision [53], sulfamic acid treatment [54], carboxylation using succinic anhydride [55], and a combination of chemical and mechanical treatments using 2,2,6,6-tetramethylpiperidine-1-oxyl radical (TEMPO)-mediated oxidation [56]. High-strength materials can be developed when cellulose nanofibers are aligned; however, cellulose microfibrils from terrestrial plants are extremely difficult to reorient after they have been individually dispersed in water. Bottom-up approaches use nanofibers to develop cellulosic materials that are inspired by the optimal microfibril orientation in the cell wall layer [57, 58], although perfectly imitating nature is difficult. Alternatively, top-down approaches have been proposed, in which the non-cellulosic components are removed while maintaining the hierarchical structure of the woody biomass.

In order to develop a novel material based on cellulose microfibrils supported by the hierarchical wood structure, researchers have examined top-down approaches that remove matrix components. Yano et al. reported the partial removal of lignin using NaClO_2 followed by treatment with NaOH, and then impregnation with resin to obtain a high-strength wood [59]. Delignified and densified wood has been reported to exhibit excellent mechanical anisotropy [60, 61]. Optically transparent wood was first reported in 1992 by Fink [62], and recently it was also produced by delignification with NaClO_2 followed by impregnation with prepolymerized methyl

methacrylate [63]. Additional techniques for producing transparent wood have also been reported (e.g., solar-assisted chemical brushing [64] and UV irradiation [65]). The combination of delignification using boiling aqueous $\text{NaOH}/\text{Na}_2\text{SO}_3$ with hot pressing results in remarkably strong densified wood as well [66]. The selective separation of oil/water mixtures using strong, mesoporous, and hydrophobic biocomposites is a recent application that has been explored [67, 68].

By detailed monitoring of wood delignification using IR spectroscopy [69], our group fabricated a novel cellulose block with the natural architecture of wood through alcoholysis with ethylene glycol combined with NaClO_2 [70]. Figure 1 shows a representative colorless wood block prepared using the two-step delignification process and a schematic model of the hierarchical structure of wood with the corresponding morphological and structural data obtained from different analytical techniques. This delignified wood is unique in that most of the hemicellulose has also been removed. Author and co-workers have further improved the technique and demonstrated its applicability to bamboo [71]. In addition, non-cellulosic components were removed from wood blocks by changing the treatment conditions to generate cellulose blocks with varying degrees of polymerization while maintaining the anatomical structure [72]. The microfibril sheets oriented by heat-pressing exhibited desirable physical properties (Fig. 2), with the specific modulus independent of the degree of polymerization as long as the orientation was maintained. In contrast, the tensile strength of the oriented sheet varied with the degree of polymerization, which highlights the notable influence of single fiber strength compared to the randomly oriented sheet. Lignin-free wood blocks, which are supported by the three-dimensional (3D) architecture of wood, have great potential as new materials, which can also be used to understand the formation and functionality of the structure of wood.

Conclusion

Primitive organisms such as bacteria and sea algae synthesize relatively large cellulose fibers. In contrast, terrestrial plants generate small microfibrils, possibly to increase their surface area and facilitate interactions with matrix components, such as lignin and hemicellulose, which helps their survival under harsh environmental conditions. Given the long history of trees on Earth, the complex 3D structure of wood underpinned by cellulose provides the exemplary structure as a high-strength material. Consequently, new functional materials with guaranteed strengths may be developed using colorless wood as a framework and injecting matrix components

other than lignin. In addition, incorporating selective lignin polymerization technology into colorless wood [73] may further clarify the relationship between the chemical composition and physical properties of wood.

Abbreviations

IR: Infrared; NMR: Nuclear magnetic resonance; TEMPO: 2,2,6,6-Tetramethylpiperidine-1-oxyl.

Acknowledgements

The author thanks Mr. Adachi of Kyoto University for providing wood samples, and Mr. Seiya Hirano, Ms. Rino Tsushima, and Mr. Tatsuki Kurei of Tokyo University of Agriculture and Technology for support related to data collection and analysis provided for some of the work reported herein. Finally, I express my sincere gratitude to Prof. Junji Sugiyama of Kyoto University for providing the opportunity to study cellulose and wood science.

Author contributions

YH conceptualized the research, conducted a literature review, and wrote the manuscript. The author read and approved the final manuscript.

Funding

Some of the work reported herein was jointly supported by Grants-in-Aid for Scientific Research (KAKENHI) [Grant No. 19K06167 and 22K19203] from the Japan Society for the Promotion of Science (JSPS).

Availability of data and materials

Not applicable.

Declarations

Competing interests

The author declares no competing interests.

Received: 14 April 2022 Accepted: 29 August 2022

Published online: 15 September 2022

References

- Motaung TE, Liganiso LZ (2018) Critical review on agrowaste cellulose applications for biopolymers. *Int J Plast Technol* 22:185–216. <https://doi.org/10.1007/s12588-018-9219-6>
- Nishikawa S, Ono S (1913) Transmission of X-Rays through fibrous, lamellar and granular substances. *Proc Tokyo Math-Phys Societ* 2(7):131–138
- Meyer KH, Mark H (1928) Über den Bau des krystallisierten Anteils der Cellulose. *Ber Dtsch Chem Ges A/B* 61:593–614. <https://doi.org/10.1002/cber.19280610402>
- Meyer KH, Misch L (1937) Positions des atomes dans le nouveau modèle spatial de la cellulose. *Helv Chim Acta* 20:232–244. <https://doi.org/10.1002/hlca.19370200134>
- Honjo G, Watanabe M (1958) Examination of cellulose fibre by the low-temperature specimen method of electron diffraction and electron microscopy. *Nature* 181:326–328. <https://doi.org/10.1038/181326a0>
- Marrinan HJ, Mann J (1956) Infrared spectra of the crystalline modifications of cellulose. *J Polym Sci* 21:301–311. <https://doi.org/10.1002/pol.1956.120219812>
- Mann J, Marrinan HJ (1958) Crystalline modifications of cellulose. Part II. A study with plane-polarized infrared radiation. *J Polym Sci* 32:357–370. <https://doi.org/10.1002/pol.1958.1203212507>
- Fisher DG, Mann J (1960) Crystalline modifications of cellulose. Part VI. Unit cell and molecular symmetry of cellulose I. *J Polym Sci* 42:189–194. <https://doi.org/10.1002/pol.1960.1204213921>
- Sarko A, Muggli R (1974) Packing analysis of carbohydrates and polysaccharides. III Valonia cellulose and cellulose II. *Macromolecules* 7:486–494. <https://doi.org/10.1021/ma00040a016>
- Gardner KH, Blackwell J (1974) The structure of native cellulose. *Biopolymers* 13:1975–2001. <https://doi.org/10.1002/bip.1974.360131005>
- Atalla RH, VanderHart DL (1984) Native cellulose: a composite of two distinct crystalline forms. *Science* 223:283–285. <https://doi.org/10.1126/science.223.4633.283>
- VanderHart DL, Atalla RH (1984) Studies of microstructure in native celluloses using solid-state carbon-13 NMR. *Macromolecules* 17:1465–1472. <https://doi.org/10.1021/ma00138a009>
- Yamamoto H, Horii F, Odani H (1989) Structural changes of native cellulose crystals induced by annealing in aqueous alkaline and acidic solutions at high temperatures. *Macromolecules* 22:4130–4132. <https://doi.org/10.1021/ma00200a058>
- Debzi EM, Chanzy H, Sugiyama J, Tekely P, Excoffier G (1991) The $\text{I}\alpha \rightarrow \text{I}\beta$ transformation of highly crystalline cellulose by annealing in various mediums. *Macromolecules* 24:6816–6822. <https://doi.org/10.1021/ma00026a002>
- Sugiyama J, Vuong R, Chanzy H (1991) Electron diffraction study on the two crystalline phases occurring in native cellulose from an algal cell wall. *Macromolecules* 24:4168–4175. <https://doi.org/10.1021/ma00014a033>
- Nishiyama Y, Langan P, Chanzy H (2002) Crystal structure and hydrogen-bonding system in cellulose $\text{I}\beta$ from synchrotron X-ray and neutron fiber diffraction. *J Am Chem Soc* 124:9074–9082. <https://doi.org/10.1021/ja0257319>
- Nishiyama Y, Sugiyama J, Chanzy H, Langan P (2003) Crystal structure and hydrogen bonding system in cellulose $\text{I}\alpha$ from synchrotron X-ray and neutron fiber diffraction. *J Am Chem Soc* 125:14300–14306. <https://doi.org/10.1021/ja037055w>
- Sugiyama J, Persson J, Chanzy H (1991) Combined infrared and electron diffraction study of the polymorphism of native celluloses. *Macromolecules* 24:2461–2466. <https://doi.org/10.1021/ma00009a050>
- Wada M, Sugiyama J, Okano T (1993) Native celluloses on the basis of two crystalline phase ($\text{I}\alpha/\text{I}\beta$) system. *J Appl Polym Sci* 49:1491–1496. <https://doi.org/10.1002/app.1993.070490817>
- Nakashima K, Nishino A, Horikawa Y, Hirose E, Sugiyama J, Satoh N (2011) The crystalline phase of cellulose changes under developmental control in a marine chordate. *Cell Mol Life Sci* 68:1623–1631. <https://doi.org/10.1007/s00018-010-0556-7>
- Horikawa Y (2017) Assessment of cellulose structural variety from different origins using near infrared spectroscopy. *Cellulose* 24:5313–5325. <https://doi.org/10.1007/s10570-017-1518-0>
- Wang H, Tsuchikawa S, Inagaki T (2021) Terahertz time-domain spectroscopy as a novel tool for crystallographic analysis in cellulose: the potentiality of being a new standard for evaluating crystallinity. *Cellulose* 28:5293–5304. <https://doi.org/10.1007/s10570-021-03902-x>
- Imai T, Sugiyama J (1998) Nanodomains of $\text{I}\alpha$ and $\text{I}\beta$ cellulose in algal microfibrils. *Macromolecules* 31:6275–6279. <https://doi.org/10.1021/ma980664h>
- Yamamoto H, Horii F, Hirai A (1996) In situ crystallization of bacterial cellulose II. Influences of different polymeric additives on the formation of celluloses $\text{I}\alpha$ and $\text{I}\beta$ at the early stage of incubation. *Cellulose* 3:229–242. <https://doi.org/10.1007/BF02228804>
- Wada M, Okano T (2001) Localization of $\text{I}\alpha$ and $\text{I}\beta$ phases in algal cellulose revealed by acid treatments. *Cellulose* 8:183–188. <https://doi.org/10.1023/A:1013196220602>
- Hayashi N, Sugiyama J, Okano T, Ishihara M (1997) Selective degradation of the cellulose $\text{I}\alpha$ component in *Cladophora* cellulose with *Trichoderma viride* cellulase. *Carbohydr Res* 305:109–116. [https://doi.org/10.1016/S0008-6215\(97\)00281-4](https://doi.org/10.1016/S0008-6215(97)00281-4)
- Hayashi N, Sugiyama J, Okano T, Ishihara M (1997) The enzymatic susceptibility of cellulose microfibrils of the algal-bacterial type and the cotton-ramie type. *Carbohydr Res* 305:261–269. [https://doi.org/10.1016/S0008-6215\(97\)10032-5](https://doi.org/10.1016/S0008-6215(97)10032-5)
- Hayashi N, Kondo T, Ishihara M (2005) Enzymatically produced nano-ordered short elements containing cellulose $\text{I}\beta$ crystalline domains. *Carbohydr Polym* 61:191–197. <https://doi.org/10.1016/j.carbpol.2005.04.018>
- Hackney JM, Atalla RH, Vanderhart DL (1994) Modification of crystallinity and crystalline structure of *Acetobacter xylinum* cellulose in the presence of water-soluble β -1,4-linked polysaccharides: ^{13}C -NMR evidence. *Int J Biol Macromol* 16:215–218. [https://doi.org/10.1016/0141-8130\(94\)90053-1](https://doi.org/10.1016/0141-8130(94)90053-1)

30. Goto T, Harada H, Saeki H (1973) Cross-sectional view of microfibrils in *Valonia* (*Valonia macrophysa*). Mokuzai Gakkaishi 19:463–468
31. Revol J-F (1982) On the cross-sectional shape of cellulose crystallites in *Valonia ventricosa*. Carbohydr Polym 2:123–134. [https://doi.org/10.1016/0144-8617\(82\)90058-3](https://doi.org/10.1016/0144-8617(82)90058-3)
32. Sugiyama J, Harada H, Fujiyoshi Y, Ueda N (1984) High resolution observations of cellulose microfibrils. Mokuzai Gakkaishi 30:98–99
33. Imai T, Sugiyama J, Itoh T, Horii F (1999) Almost pure I_a cellulose in the cell wall of *Glaucozystis*. J Struct Biol 127:248–257. <https://doi.org/10.1006/jsbi.1999.4160>
34. Kim NH, Herth W, Vuong R, Chanzy H (1996) The cellulose system in the cell wall of *Micrasterias*. J Struct Biol 117:195–203. <https://doi.org/10.1006/jsbi.1996.0083>
35. Van Daele Y, Revol JF, Gaill F, Goffinet G (1992) Characterization and supramolecular architecture of the cellulose-protein fibrils in the tunic of the sea peach (*Halocynthia papillosa*, Ascidiacea, Urochordata). Biol Cell 76:87–96. [https://doi.org/10.1016/0248-4900\(92\)90198-A](https://doi.org/10.1016/0248-4900(92)90198-A)
36. Goto T, Harada H, Saeki H (1975) Cross-sectional view of microfibrils in gelatinous layer of poplar tension wood (*Populus euramericana*). Mokuzai Gakkaishi 21:537–542
37. Fernandes AN, Thomas LH, Altaner CM, Callowd P, Forsyth VT, Apperley DC, Kennedy CJ, Jarvis MC (2011) Nanostructure of cellulose microfibrils in spruce wood. Proc Natl Acad Sci USA 108:E1195–E1203. <https://doi.org/10.1073/pnas.1108942108>
38. Newman RH, Hill SJ, Harris PJ (2013) Wide-angle X-ray scattering and solid-state nuclear magnetic resonance data combined to test models for cellulose microfibrils in mung bean cell walls. Plant Physiol 163:1558–1567. <https://doi.org/10.1104/pp.113.228262>
39. Daicho K, Saito T, Fujisawa S, Isogai A (2018) The crystallinity of nanocellulose: Dispersion-induced disordering of the grain boundary in biologically structured cellulose. ACS Appl Nano Mater 1:5774–5785. <https://doi.org/10.1021/acsanm.8b01438>
40. Liang CY, Marchessault RH (1960) Infrared spectra of crystalline polysaccharides. IV. The use of inclined incidence in the study of oriented films. J Polym Sci 43:85–100. <https://doi.org/10.1002/pol.1960.1204314108>
41. Kregger DR (1957) New crystallite orientations of cellulose I in *Spirogyra* cell-walls. Nature 180:914–915. <https://doi.org/10.1038/180914a0>
42. Koyama M, Sugiyama J, Itoh T (1997) Systematic survey on crystalline features of algal celluloses. Cellulose 4:147–160. <https://doi.org/10.1023/a:1018427604670>
43. Frilette VJ, Hanle J, Mark H (1948) Rate of exchange of cellulose with heavy water. J Am Chem Soc 70:1107–1113. <https://doi.org/10.1021/ja01183a071>
44. Wada M, Okano T, Sugiyama J (1997) Synchrotron-radiated X-ray and neutron diffraction study of native cellulose. Cellulose 4:221–232. <https://doi.org/10.1023/A:1018435806488>
45. Nishiyama Y, Isogai A, Okano T, Müller M, Chanzy H (1999) Intracrystalline deuteration of native cellulose. Macromolecules 32:2078–2081. <https://doi.org/10.1021/ma981563m>
46. Horikawa Y, Sugiyama J (2008) Accessibility and size of *Valonia* cellulose microfibril studied by combined deuteration/rehydrogenation and FTIR technique. Cellulose 15:419–424. <https://doi.org/10.1007/s10570-007-9187-z>
47. Horikawa Y, Clair B, Sugiyama J (2009) Varietal difference in cellulose microfibril dimensions observed by infrared spectroscopy. Cellulose 16:1–8. <https://doi.org/10.1007/s10570-008-9252-2>
48. Horikawa Y, Itoh T, Sugiyama J (2006) Preferential uniplanar orientation of cellulose microfibrils reinvestigated by the FTIR technique. Cellulose 13:309–316. <https://doi.org/10.1007/s10570-005-9037-9>
49. Horikawa Y (2009) Sugiyama J Localization of crystalline allomorphs in cellulose microfibril. Biomacromol 10:2235–2239. <https://doi.org/10.1021/bm900413k>
50. Funahashi R, Okita Y, Hondo H, Zhao M, Saito T, Isogai A (2017) Different conformations of surface cellulose molecules in native cellulose microfibrils revealed by layer-by-layer peeling. Biomacromol 18:3687–3694. <https://doi.org/10.1021/acs.biomac.7b01173>
51. Isogai A (2015) Structural characterization and modifications of surface-oxidized cellulose nanofiber. J Jpn Petrol Inst 58:365–375. <https://doi.org/10.1627/jpi.58.365>
52. Abe K, Iwamoto S, Yano H (2007) Obtaining cellulose nanofibers with a uniform width of 15 nm from wood. Biomacromol 8:3276–3278. <https://doi.org/10.1021/bm700624p>
53. Kose R, Mitani I, Kasai W, Kondo T (2011) 'Nanocellulose' as a single nanofiber prepared from pellicle secreted by *Gluconacetobacter xylinus* using aqueous counter collision. Biomacromol 12:716–720. <https://doi.org/10.1021/bm1013469>
54. Briois B, Saito T, Pétrier C, Putaux J-L, Nishiyama Y, Heux L, Molina-Boisseau S (2013) I_a → I_β transition of cellulose under ultrasonic radiation. Cellulose 20:597–603. <https://doi.org/10.1007/s10570-013-9866-x>
55. Sehaqui H, Kulasinski OK, Pfenninger ON, Zimmermann T, Tingaut P (2017) Highly carboxylated cellulose nanofibers via succinic anhydride esterification of wheat fibers and facile mechanical disintegration. Biomacromol 18:242–248. <https://doi.org/10.1021/acs.biomac.6b01548>
56. Saito T, Kimura S, Nishiyama Y, Isogai A (2007) Cellulose nanofibers prepared by TEMPO-mediated oxidation of native cellulose. Biomacromol 8:2485–2491. <https://doi.org/10.1021/bm0703970>
57. Kobayashi Y, Saito T, Isogai A (2014) Aerogels with 3D ordered nanofiber skeletons of liquid-crystalline nanocellulose derivatives as tough and transparent insulators. Angew Chem Int Ed Engl 53:10394–10397. <https://doi.org/10.1002/anie.201405123>
58. Nechyporchuk O, Håkansson KMO, Gowda VK, Lundell F, Hagström B, Köhnke T (2019) Continuous assembly of cellulose nanofibers and nanocrystals into strong macrofibers through microfluidic spinning. Adv Mater Technol 4:1–10. <https://doi.org/10.1002/admt.201800557>
59. Yano H, Hirose A, Collins PJ, Yazaki Y (2001) Effects of the removal of matrix substances as a pretreatment in the production of high strength resin impregnated wood based materials. J Mater Sci Lett 20:1125–1126. <https://doi.org/10.1023/A:1010992307614>
60. Jakob M, Gaugeler J, Gindl-Altmutter W (2020) Effects of fiber angle on the tensile properties of partially delignified and densified wood. Materials (Basel) 13:5405. <https://doi.org/10.3390/ma13235405>
61. Frey M, Widner D, Segmehl JS, Casdorff K, Keplinger T, Burgert I (2018) Delignified and densified cellulose bulk materials with excellent tensile properties for sustainable engineering. ACS Appl Mater Interfaces 10:5030–5037. <https://doi.org/10.1021/acsami.7b18646>
62. Fink S (1992) Transparent wood—a new approach in the functional study of wood structure. Holzforschung 46:403–408. <https://doi.org/10.1515/hfsg.1992.46.5.403>
63. Li YY, Fu QL, Yu S, Yan M, Berglund L (2016) Optically transparent wood from a nanoporous cellulosic template: Combining functional and structural performance. Biomacromol 17:1358–1364. <https://doi.org/10.1021/acs.biomac.6b00145>
64. Xia Q, Chen C, Li T, He S, Gao J, Wang X, Hu L (2021) Solar-assisted fabrication of large-scale, patternable transparent wood. Sci Adv. <https://doi.org/10.1126/sciadv.abd7342>
65. Samanta A, Chen H, Samanta P, Popov S, Sychugov I, Berglund LA (2021) Reversible dual-stimuli-responsive chromic transparent wood biocomposites for smart window applications. ACS Appl Mater Interfaces 13:3270–3277. <https://doi.org/10.1021/acsami.0c21369>
66. Song JW, Chen CJ, Zhu SZ, Zhu MW, Dai JQ, Ray U, Li YJ, Kuang YD, Li YF, Quispe N, Yao YG, Gong A, Leiste UH, Bruck HA, Zhu JY, Vellore A, Li H, Minus ML, Jia Z, Martini A, Li T, Hu LB (2018) Processing bulk natural wood into a high-performance structural material. Nature 554:224–228. <https://doi.org/10.1038/nature25476>
67. Fu Q, Ansari F, Zhou Q, Berglund LA (2018) Wood nanotechnology for strong, mesoporous, and hydrophobic biocomposites for selective separation of oil/water mixtures. ACS Nano 12:2222–2230. <https://doi.org/10.1021/acs.nano.8b00005>
68. Wang K, Liu X, Tan Y, Zhang W, Zhang S, Li J (2019) Two-dimensional membrane and three-dimensional bulk aerogel materials via top-down wood nanotechnology for multibehavioral and reusable oil/water separation. Chem Eng J 371:769–780. <https://doi.org/10.1016/j.cej.2019.04.108>
69. Horikawa Y, Hirano S, Mihashi A, Kobayashi Y, Zhai S, Sugiyama J (2019) Prediction of lignin contents from infrared spectroscopy: chemical digestion and lignin/biomass ratios of *Cryptomeria japonica*. Appl Biochem Biotechnol 188:1066–1076. <https://doi.org/10.1007/s12010-019-02965-8>
70. Horikawa Y, Tsushima R, Noguchi K, Nakaba S, Funada R (2020) Development of colorless wood via two-step delignification involving alcoholysis and bleaching with maintaining natural hierarchical structure. J Wood Sci 66:37. <https://doi.org/10.1186/s10086-020-01884-1>

71. Kurei T, Tsushima R, Okahisa Y, Nakaba S, Funada R, Horikawa Y (2021) Creation and structural evaluation of the three-dimensional cellulosic material "White-Colored Bamboo." *Holzforschung* 75:180–186. <https://doi.org/10.1515/hf-2020-0030>
72. Kurei T, Hioki Y, Kose R, Nakaba S, Funada R, Horikawa Y (2021) Effects of orientation and degree of polymerization on tensile properties in the cellulose sheets using hierarchical structure of wood. *Cellulose* 29:2885–2898. <https://doi.org/10.1007/s10570-021-04160-7>
73. Hirano S, Yamagishi Y, Nakaba S, Kajita S, Funada R, Horikawa Y (2020) Artificially lignified cell wall catalyzed by peroxidase selectively localized on a network of microfibrils from cultured cells. *Planta* 251:104. <https://doi.org/10.1007/s00425-020-03396-0>

Publisher's Note

Springer Nature remains neutral with regard to jurisdictional claims in published maps and institutional affiliations.

Submit your manuscript to a SpringerOpen[®] journal and benefit from:

- Convenient online submission
- Rigorous peer review
- Open access: articles freely available online
- High visibility within the field
- Retaining the copyright to your article

Submit your next manuscript at ► [springeropen.com](https://www.springeropen.com)